Nuclear shape and structure in neutron-rich ^{110,111}Tc

Y. X. Luo,[1,2] J. H. Hamilton,[1] J. O. Rasmussen,[2] A. V. Ramayya,[1] I. Stefanescu,[3] J. K. Hwang,[1] X. L. Che,[4] S. J. Zhu,[1,4,5] P. M. Gore,[1] E. F. Jones,[1] D. Fong,[1] S. C. Wu,[6] I. Y. Lee,[2] T. N. Ginter,[2,7] W. C. Ma,[8] G. M. Ter-Akopian,[9] A. V. Daniel,[9] M. A. Stoyer,[10] R. Donangelo,[11] and A. Gelberg[12]

[1]*Physics Department, Vanderbilt University, Nashville, Tennessee 37235, USA*
[2]*Lawrence Berkeley National Laboratory, Berkeley, California 94720, USA*
[3]*KU Leuven, Instituut voor Kern- en Stralingsfysica, Celestijnenlaan 200D, B-3001 Leuven, Belgium*
[4]*Physics Department, Tsinghua University, Beijing 100084, China*
[5]*Joint Institute for Heavy Ion Research, Oak Ridge, Tennessee 37831, USA*
[6]*Department of Physics, National Tsing Hua University, Hsinchu, Taiwan*
[7]*National Superconducting Cyclotron Laboratory, Michigan State University, East Lansing, Michigan 48824, USA*
[8]*Mississippi State University, Drawer 5167, Mississippi State, Mississippi 39762, USA*
[9]*Flerov Laboratory for Nuclear Reactions, JINR, Dubna, Russia*
[10]*Lawrence Livermore National Laboratory, Livermore, California 94550, USA*
[11]*Universidade Federal do Rio de Janeiro, CP 68528, RG Brazil*
[12]*Institut für Kernphysik, Universität zu Köln, D-50937, Köln, Germany*

(Received 27 February 2006; revised manuscript received 11 May 2006; published 18 August 2006)

The high-spin nuclear structure of Tc isotopes is extended to more neutron-rich regions based on the measurements of prompt γ rays from the spontaneous fission of ^{252}Cf at the Gammasphere. The high-spin level scheme of $N = 67$ neutron-rich ^{110}Tc ($Z = 43$) is established for the first time, and that of ^{111}Tc is extended and expanded. The ground band of ^{111}Tc reaches the band-crossing region, and the new observation of the weakly populated $\alpha = -1/2$ member of the band provides important information on signature splitting. The systematics of band crossings in the isotopic and isotonic chains and a CSM calculation suggest that the band crossing of the ground band of ^{111}Tc is due to alignment of a pair of $h_{11/2}$ neutrons. The best fit to signature splitting, branching ratios, and excitations of the ground band of ^{111}Tc by the rigid triaxial rotor plus particle model calculations result in a shape of $\varepsilon_2 = 0.32$ and $\gamma = -26^\circ$ for this nucleus. Its triaxiality is larger than that of ^{107,109}Tc, which indicates increasing triaxiality in Tc isotopes with increasing neutron number. The identification of the weakly populated $K+2$ satellite band provides strong evidence for the large triaxiality of ^{111}Tc. In ^{110}Tc, the four lowest-lying levels observed are very similar to those in ^{108}Tc. At an excitation of 478.9 keV above the lowest state observed, ten states of a $\Delta I = 1$ band are observed. This band of ^{110}Tc is very analogous to the $\Delta I = 1$ bands in ^{106,108}Tc, but it has greater and reversal signature splitting at higher spins.

DOI: 10.1103/PhysRevC.74.024308 PACS number(s): 21.10.−k, 27.60.+j, 25.85.Ca, 21.60.Cs

I. INTRODUCTION

The studies of shape coexistence and shape transitions in the neutron-rich $A \sim 100$ region have long been of major interest [1,2]. In this region, shape transitions from spherical to strongly deformed shapes are observed along the $Z \sim 40$ isotopic chains, and quadrupole deformations are found to decrease with increasing proton number between 38 and 42 [3–6]. Our systematic studies of neutron-rich odd-Z Y-Nb-Tc-Rh (Z = 39-41-43-45) isotopes identified a shape transition from an axially symmetric shape with very large quadrupole deformations in ^{99,101}Y to large triaxial deformations in ^{107,109}Tc and ^{111,113}Rh isotopes [7–9].

It is of interest to explore further their structure along isotopic chains to the more neutron-rich region. For Rh ($Z = 45$) isotopes, $N = 67$ isotope ^{112}Rh and $N = 68$ isotope ^{113}Rh have been reached [7]. For Tc ($Z = 43$) isotopes, however, although the heavy $N = 72$ isotope ^{115}Tc was observed by using a projectile fragmentation technique [10], the high-spin structure of Tc isotopes was available only up to the $N = 66$ isotope ^{109}Tc [8,11]. In the previous studies of lighter Tc isotopes, high-spin level schemes were established and a shift from a weak-coupling scheme toward a strong-coupling scheme from ^{97}Tc to ^{105}Tc was reported [12]. Afterward, the strong-coupling scheme and large signature splitting were extended to ^{107,109}Tc [8,11]. This evolution of coupling schemes was interpreted as due to the location of the Fermi level changing with deformation as the neutron number increases [8,10]. The proton Fermi level, being close to $1/2^+$ and $3/2^+$ of the $\pi g_{9/2}$ subshell for ^{97,99}Tc with small deformations, approaches the $5/2^+$ of the same subshell for $^{103-109}$Tc with larger deformations. A quadrupole deformation $\varepsilon_2 = 0.32$ and triaxiality $\gamma = -22.5^\circ$ were deduced in ^{107}Tc [8].

In the present paper, we report new experimental results obtained for the high-spin structure of the $N = 67$ isotope ^{110}Tc and $N = 68$ isotope ^{111}Tc, which were achieved at almost the same time as we identified for the first time the high-spin level scheme of ^{138}Cs [13]. No low-lying yrast cascade had been reported in ^{110,111}Tc before the present work. Seven non-yrast levels up to a low excitation energy of 740.8 keV in ^{110}Tc were reported in Nuclear Data Sheets [14] by measurements of ^{110}Mo β^- decay. In the present paper, the high-spin level scheme of ^{110}Tc is proposed for the first time,

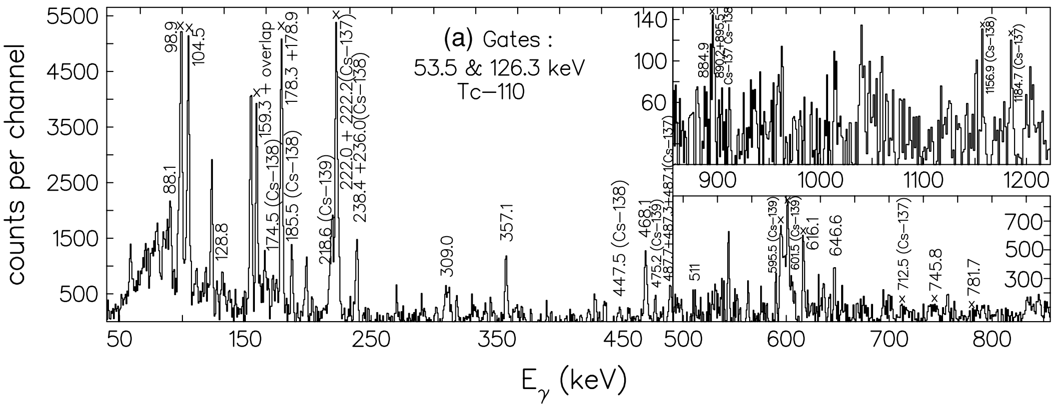

FIG. 1(a). Double-gated triple-coincidence spectrum for ^{110}Tc data analysis. Gates are set on the 53.5 and 126.3 keV transitions of ^{110}Tc. All transitions identified in ^{110}Tc coincident with the gates are simultaneously seen in the spectrum with those of the complementary fission partners ^{137,138,139}Cs.

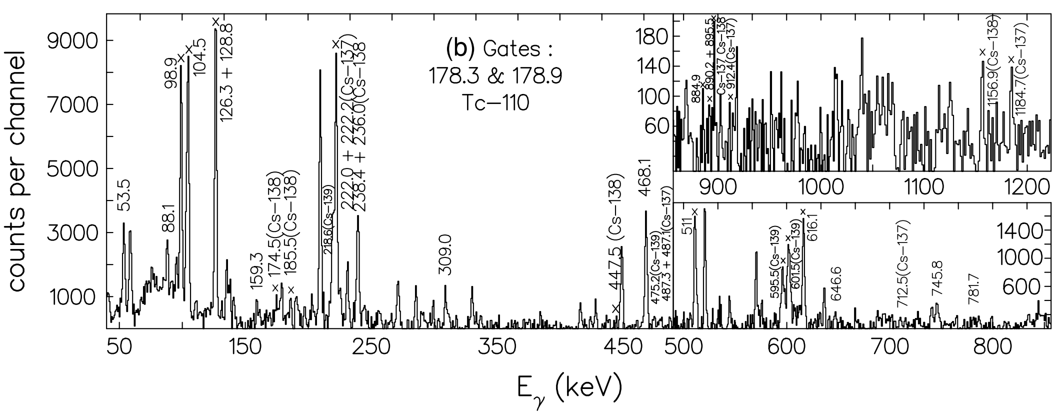

FIG. 1(b). Same as Fig. 1(a), but gates are set on the 178.3 and 178.9 keV transitions of ^{110}Tc.

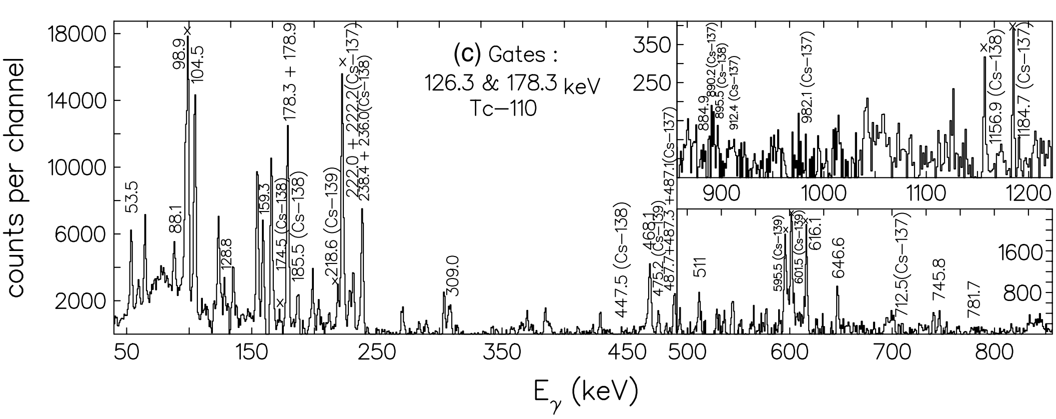

FIG. 1(c). Same as Fig. 1(a), but gates are set on the 126.3 and 178.3 keV transitions of ^{110}Tc.

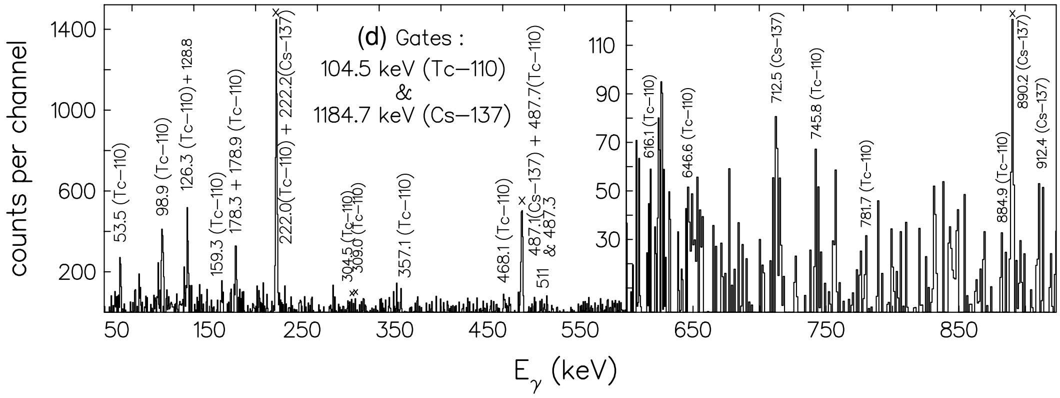

FIG. 1(d). Same as Fig. 1(a), but one of the gates is set on the 104.5 keV transition of ^{110}Tc and the other on the 1184.7 keV transition of ^{137}Cs. Transitions of the 5n fission partner pair ^{110}Tc-^{137}Cs are simultaneously seen.

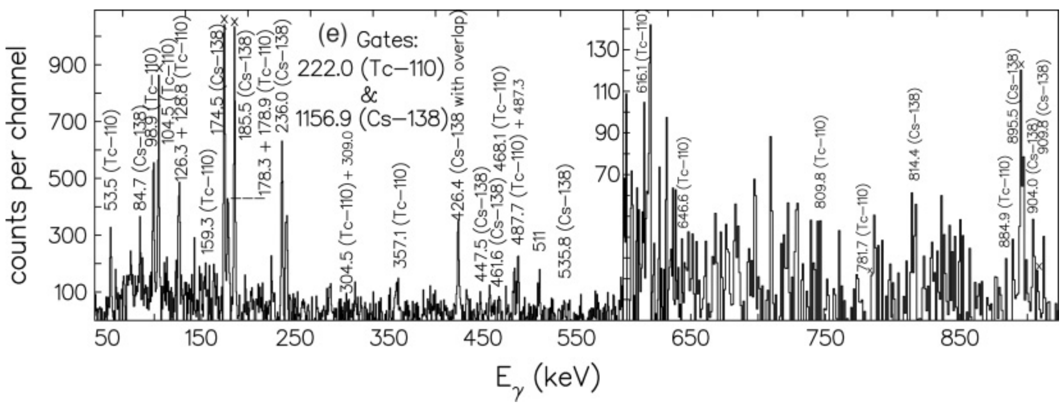

FIG. 1(e). Same as Fig. 1(a), but one of the gates is set on the 222.0 keV transition of ^{110}Tc and the other on the 1156.9 keV transition of ^{138}Cs. Transitions of the 4n fission partner pair ^{110}Tc-^{138}Cs are simultaneously seen. This gated spectrum provides more evidence for the identifications of the 222.0 and 487.7 keV transition of ^{110}Tc which are, respectively, overlapped by the 222.2 and 487.1 keV transition of the 5n fission partner ^{137}Cs.

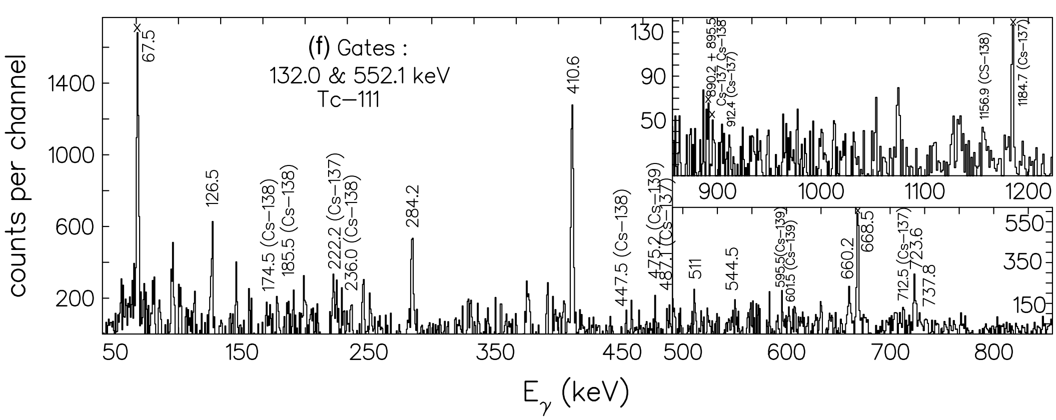

FIG. 1(f). Same as Fig. 1(a), but gates are set on the 132.0 and 552.1 keV transitions of ^{111}Tc.

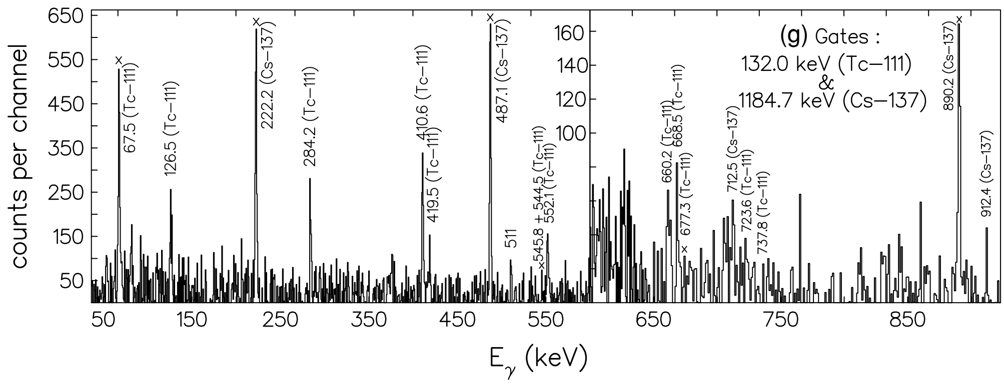

FIG. 1(g). Same as Fig. 1(a), but one of the gates is set on the 132.0 keV transition of ^{111}Tc and the other on the 1184.7 keV transition of ^{137}Cs. Transitions of the 4*n* fission partner pair ^{111}Tc-^{137}Cs are simultaneously seen. Some newly observed transitions in ^{111}Tc, which, however, are not coincident with the gates and thus do not show up in Fig. 1(f), can be seen in this gated spectrum.

which reports the newly observed yrast and near-yrast levels of the nucleus. After we completed the work of both ^{110,111}Tc, a paper on ^{111}Tc was published by Urban *et al.* [15], which reported a less extended level scheme of ^{111}Tc (see Sec. II for details).

Comparison and discussion are made in the present paper for the lowest levels and the $\Delta I = 1$ yrast band of ^{110}Tc observed in the present work and those in ^{106,108}Tc [16]. The former shows an overall similarity to the latter for low-lying levels and a sharp increase and reversal in the signature splitting compared to ^{106,108}Tc [16] for higher spin levels, implying probably a significant increase in triaxiality in ^{110}Tc. Model calculations performed for ^{111}Tc are presented. The extension of the ground band and the observation of the band crossing in this band of ^{111}Tc allow the study of systematics of band crossing of Tc isotopes. The systematics of the band crossing frequencies of the Tc isotopes and cranking shell model (CSM) calculations performed in the present work for ^{111}Tc suggest that this band crossing is caused by alignment of an $h_{11/2}$ neutron pair. The observation of the weakly populated $\alpha = -1/2$ member of the ground band of ^{111}Tc provides important information on signature splitting in this nucleus. The rigid triaxial rotor plus particle (RTRP) model is employed to calculate the signature splitting, excitation energies, and branching ratios of the ground band of ^{111}Tc. The best fits of the RTRP calculation to the experiments for ^{111}Tc result in a shape of $\varepsilon_2 = 0.32$ and $\gamma = -26°$, a larger triaxiality than those in the lighter Tc isotopes, indicating an increase of triaxiality in Tc with increasing neutron number.

II. EXPERIMENTAL RESULTS

The populations and detections of the high-spin levels of ^{110,111}Tc were made by using spontaneous fission and measuring the prompt γ rays emitted in a multi-γ detection array [17]. The ^{110,111}Tc were produced as complementary fission fragments of Cs isotopes. A ^{252}Cf source of 62 μCi, sandwiched between two 10 mg cm^{-2} Fe foils, was placed in an 8 cm polyethylene ball centered in the Gammasphere, which consisted of 102 Compton-suppressed Ge detectors. Over 5.7×10^{11} triple- and higher-fold events were accumulated. A RADWARE cube three-dimensional histogram was created . A less compressed RADWARE cube was also used to clarify

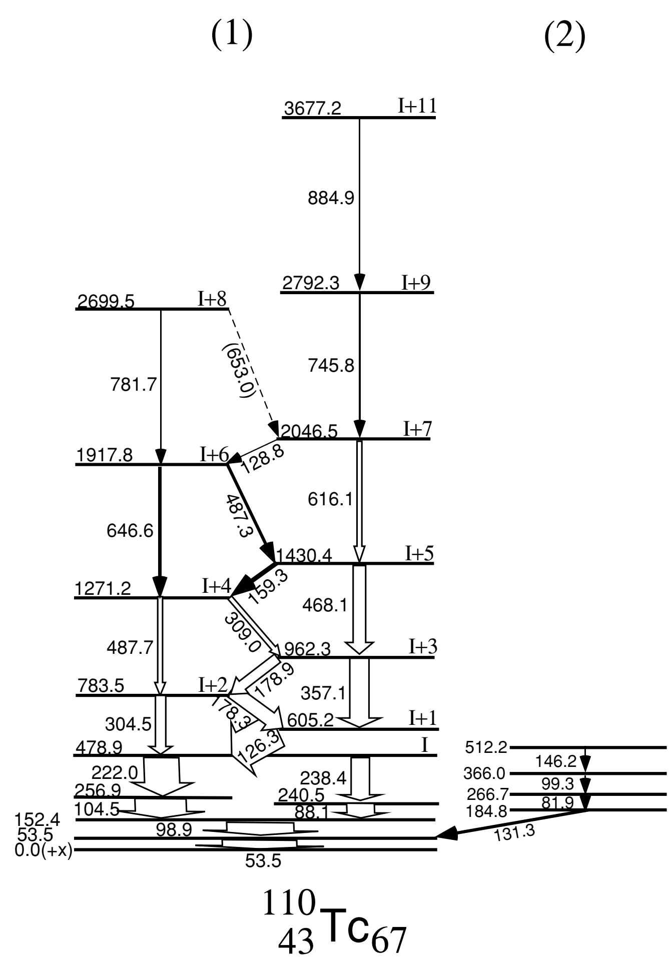

FIG. 2. High-spin level scheme of ^{110}Tc proposed for the first time in the present work, assuming bandhead spin *I*, as for ^{106,108}Tc in [16]. The coincident 53.5–131.3 keV transitions are also reported by measurements of ^{110}Mo β^- decay [14].

TABLE I. Transition energies and relative intensities of the transitions in ^{110}Tc.

E_γ (keV)	Relative intensities	E_γ^{a} (keV)	Band	Initial level (keV)
53.5		53.3	1	53.5
81.9			2	266.7
88.1			1	240.5
98.9			1	152.4
99.3			2	366.0
104.5			1	256.9
126.3	100		1	605.2
128.8	2.4		1	2046.5
131.3		131.2	2-1	184.8
146.2			2	366.0
159.3	5.1		1	1430.4
178.3	57.8		1	783.5
178.9	25.5		1	962.3
222.0	89.6		1	478.9
238.4	32.1		1	478.9
304.5	19.9		1	783.5
309.0	11.6		1	1271.2
357.1	32.2		1	962.3
468.1	24.9		1	1430.4
487.3	3.3		1	1917.8
487.7	15.0		1	1271.2
616.1	14.5		1	2046.5
646.6	7.1		1	1917.8
(650.3)			1	2699.5
745.8	3.7		1	2792.3
781.7	1.9		1	2699.5
884.9	0.5		1	3677.3

[a]Two low-lying transitions reported in [14].

TABLE II. Transition energies and relative intensities of our measured transitions in ^{111}Tc and comparison energies $E_\gamma{}^*$ from the recent work of Urban *et al.* [15].

E_γ (keV)	Relative intensities	$E_\gamma{}^*$ (keV)	Band	Initial level (keV)
67.5		67.0	1	67.5
(124.0)			1	1830.7
126.5	14.3	126.5	1	610.1
132.0	100	131.6	1	199.5
132.6	3.6		1	1162.2
284.2	26.1	284.1	1	483.7
(293.6)			6	1182.0
313.1	4.2	312.2	6	888.4
375.8	13.6	375.8	6-1	575.3
410.6	47.7	410.6	1	610.1
416.3	12.9	415.5	1	483.7
419.5	7.0		1	1029.5
(507.9)			6-1	575.3
544.5	2.6		1	1706.8
545.8	6.9		1	1029.5
552.1	28.7	552.1	1	1162.2
606.7	3.2		6	1182.0
660.2	4.3		1	3214.5
668.5	19.2	668.4	1	1271.2
677.3	2.1		1	1706.8
723.6	9.5	723.4	1	2554.3
737.8	0.7		1	3952.3

ambiguities caused by peaks overlapping, which was discussed in detail in [8].

As described in detail in our previous papers (e.g., Ref. [7]), the identifications of the transitions of ^{110,111}Tc were based on cross-checking the coincident relationships and relative transition intensities with those of the complementary fission partner Cs isotopes ^{137,138,139}Cs, and with the relevant transitions in ^{110,111}Tc as well. Careful background subtractions were always performed to eliminate possible accidental coincidences. Figures 1(a)–1(c) show typical examples of double-gated triple-coincidence spectra with both gates set on transitions in ^{110}Tc for data analysis of ^{110}Tc. Figures 1(d) and 1(e) are double-gated triple-coincidence spectra with one gate set on a transition of ^{110}Tc and the other on the ground transition of its fission partner ^{137}Cs and ^{138}Cs, respectively. In Figs. 1(a)–1(c), transitions of ^{110}Tc coincident with the gates are simultaneously seen with the transitions of all the complementary fission partner Cs isotopes. In Fig. 1(d), transitions of the 5n fission partner pair ^{110}Tc-^{137}Cs [and the transitions of the 4n fission partner pair ^{110}Tc-^{138}Cs in Fig. 1(e)] coincident with the gates are observed simultaneously. All the cross-checks showing the coincident relationship between the transitions of ^{110}Tc and the transitions of all the fission partners ^{137,138,139}Cs provide unambiguous evidence of the identification of the level scheme of ^{110}Tc. It is worth mentioning that the gated spectrum in Fig. 1(e) with one gate on the 222.0 keV transition of ^{110}Tc and the other on the 1156.9 keV transition of the 4n fission partner ^{138}Cs shows more evidence supporting the identifications of the 222.0 and 487.7 keV transitions identified in ^{110}Tc, which are overlapped by the 222.2 and 487.1 keV transitions of the 5n fission partner ^{137}Cs, respectively. Similarly, Figs. 1(f) and Fig. 1(g) show evidence of the extension of the level scheme of ^{111}Tc.

Tables I and II summarize the transition energies and relative intensities determined in the present work for all the transitions identified in ^{110,111}Tc, respectively. Those reported in [15] for ^{111}Tc and the low-lying 53.3 and 131.2 keV transitions in ^{110}Tc reported in [14] are also included in the tables.

Figures 2 and 3 show the high-spin level schemes of ^{110}Tc and ^{111}Tc proposed in the present work, respectively. Figure 2 represents the first observation of the high-spin level scheme of ^{110}Tc. The lowest 53.5 keV transition observed in ^{110}Tc is most likely the low-lying $M1$ transition of 53.3 keV reported in [14] by measurement of ^{110}Mo β^- decay. The 131.2 keV transition in coincidence with the 53.3 keV transition reported in [14] and a new weak cascade 81.9–99.3–146.2 keV above it are also identified in the present work. The observation of the low-lying 53.5–131.3 keV cascade in ^{110}Tc by both β decay [14] and by fission of ^{252}Cf in the present work thus supports the identification of the high-spin level scheme of ^{110}Tc. For ^{110}Tc, we have so far not been able to assign spins-parities to the levels observed. The levels of band 1 observed in ^{110}Tc, Fig. 2, however, are quite similar to those in ^{106,108}Tc. The

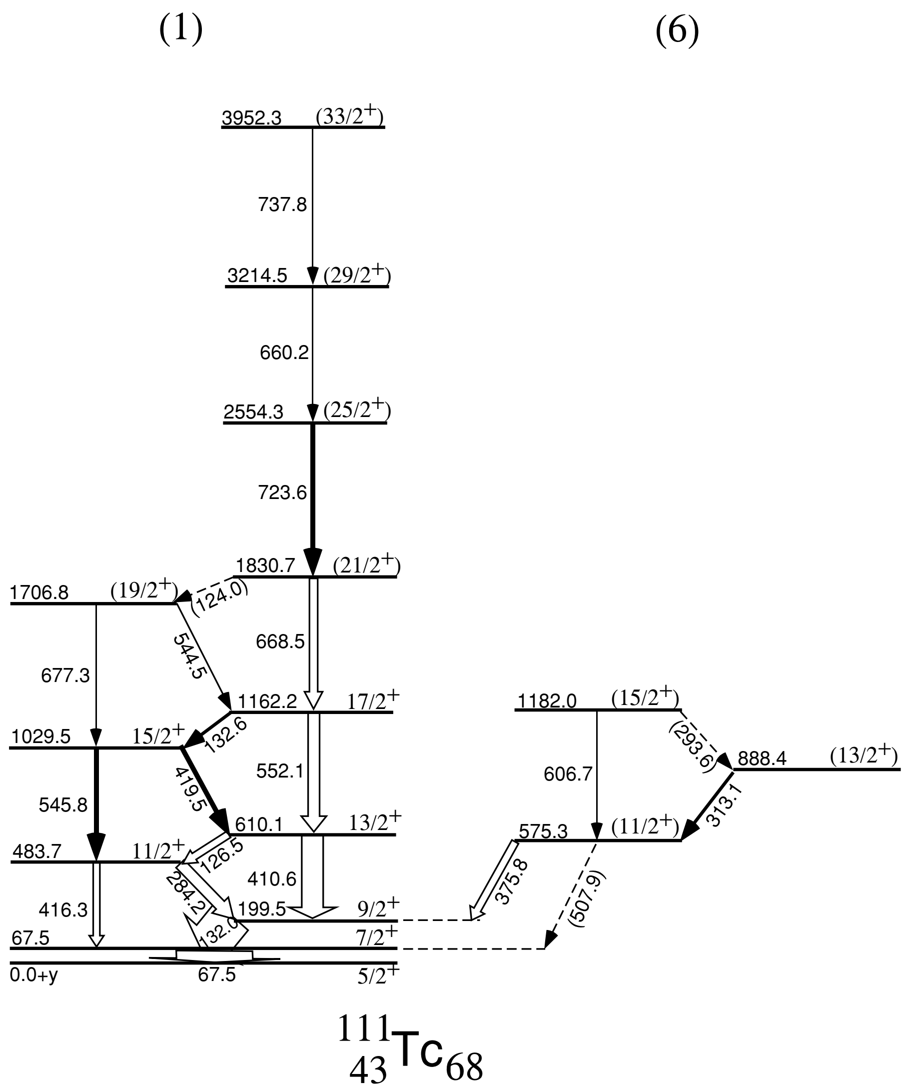

FIG. 3. High-spin level scheme of ^{111}Tc proposed in the present work. The $\alpha = +1/2$ member of the ground band reaches the band-crossing region; the weakly populated $\alpha = -1/2$ member of the ground band is identified for the first time. A $K+2$ satellite band, band 6, similar to those in ^{105,107,109}Tc [8] is also identified in ^{111}Tc.

lowest energy levels in ^{110}Tc are rather similar to those in ^{108}Tc [16]. Then at 478.9 keV above the lowest state observed, a $\Delta I = 1$ band with cascade and cross-over transitions begins that is very similar to those in ^{106,108}Tc, as shown in Fig. 4, where the level energies of these high-spin bands are compared. In Fig. 4, one also sees a change in the signature splitting of this band in ^{110}Tc compared to ^{106,108}Tc. Assuming the same bandhead spin of I for each of the three nuclei, one sees by the $I+4$ level a sharp increase and reversal in the splitting with the $I+4$ member somewhat closer to the $I+3$ level in ^{108}Tc, but the $I+4$ level is much closer to the $I+5$ level in ^{110}Tc. The splitting is also much greater in ^{110}Tc. The sharp increase in signature splitting in ^{110}Tc compared to ^{106,108}Tc may also be interpreted as a significant increase in triaxiality in ^{110}Tc.

The numbering of the bands identified in ^{111}Tc follows those for ^{105,107,109}Tc in [8]. The level scheme of ^{111}Tc is considerably more extended than that reported in [15]. The $\alpha = +1/2$ branch of the ground band (band 1) of ^{111}Tc reported in [15] reaches 2553.1 keV, (25/2$^+$) with no band-crossing observed; for the $\alpha = -1/2$ branch of band 1, only two levels at 67 and at 482.7 keV were reported in [15]. In Fig. 3, the $\alpha = +1/2$ branch of band 1 of ^{111}Tc identified in the present work reaches 3952.3 keV, (33/2$^+$) level and shows clearly a band crossing. The $\alpha = -1/2$ branch of band 1 reaches 1706.8 keV, (19/2$^+$) level, which provides important information about signature splitting of band 1. As seen in Fig. 3, the band 6 observed in ^{105,107,109}Tc [8] is also observed in ^{111}Tc.

The spin-parity assignments of the observed levels of ^{111}Tc are based on the level systematics observed in the Tc isotopic chains and on the observation of both cascade and linking transitions in the lower part of the bands. Shown in Fig. 5 are excitations of the levels of the ground $\pi g_{9/2}$ bands of ^{105,107,109,111}Tc. The smooth change of the level patterns with increasing neutron number supports the spin-parity assignments of the levels observed in ^{111}Tc (Fig. 3). It is reasonable to interpret the ground band of ^{111}Tc also as $\pi g_{9/2}$.

III. DISCUSSION AND CALCULATIONS

The extending of ground band 1 of ^{111}Tc allows a study of the systematics of band crossings in this band for the

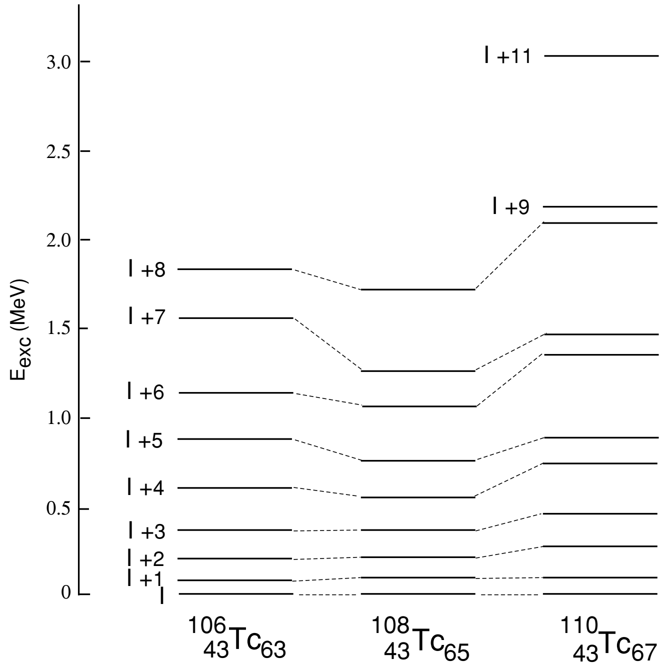

FIG. 4. Level systematics of the high-spin bands in even-A ^{106,108,110}Tc. The $\Delta I = 1$ yrast band observed in ^{110}Tc is very analogous to those recently observed in ^{106,108}Tc [16], but it has greater and reversal signature splitting at higher spins.

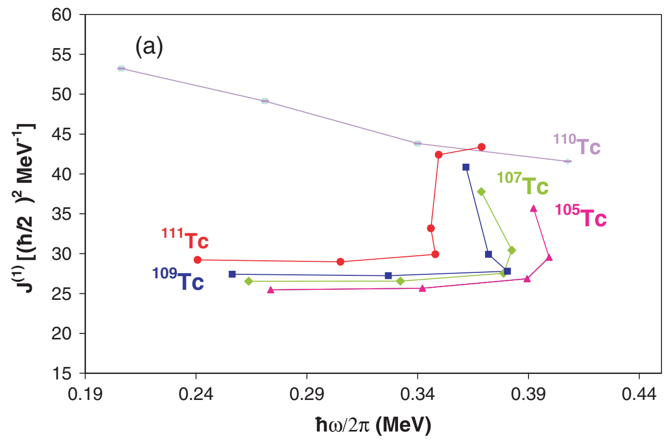

FIG. 6(a). (Color online) Kinematic moment of inertia $J^{(1)}$ of the ground bands of odd-A $^{105-111}$Tc and ^{110}Tc. Crossing frequency decreases with increasing neutron number. However, no crossing is seen in ^{110}Tc in the frequency region. Data are from the present work and [8,12].

odd-A Tc isotopes. The kinematic moment of inertias of band 1 of ^{105,107,109,110,111}Tc are given in Fig. 6(a). In the figure, a band crossing is observed in ^{111}Tc at a rotational frequency of ∼0.35 MeV, with crossing frequency decreasing with increasing neutron number for the Tc isotopes; for the odd-neutron neighbor ^{110}Tc, no band crossing is observed in the frequency region. Figure 6(b) shows $J(1)$ of the ground bands in $N = 68$ isotones ^{111}Tc and ^{113}Rh [7]. The band crossing of the ground band of ^{111}Tc is observed at almost the same rotational frequency as that of ^{113}Rh, also with no band crossing observed in the odd-neutron neighbor ^{112}Rh [7], where there is odd-neutron blocking. All the observations imply that the band crossing of the ground band of ^{111}Tc can be interpreted to have the same origin as that of ^{113}Rh, that is, the breaking of a pair of $h_{11/2}$ neutrons [7].

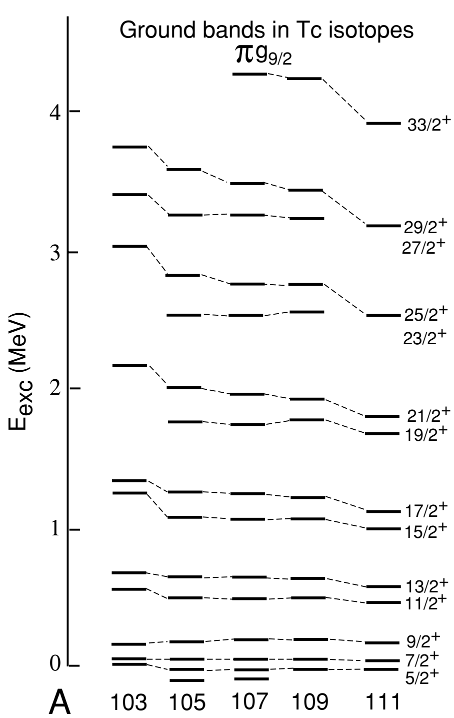

FIG. 5. Systematics of level patterns of ground bands of odd-A $^{103-111}$Tc isotopes. Data are from the present work and [8,12]. A smooth trend can be seen.

Cranking shell model (CSM) calculations described by Bengtsson and Frauendorf [19–21] were performed in the present work for ^{111}Tc to give total Routhian surface (TRS) and Routhian. The TRS calculations gave deformation parameters of $\beta_2 = 0.237, \beta_4 = -0.046, \gamma = 60^{\circ}$ at $\hbar\omega = 0.0$ MeV. It can

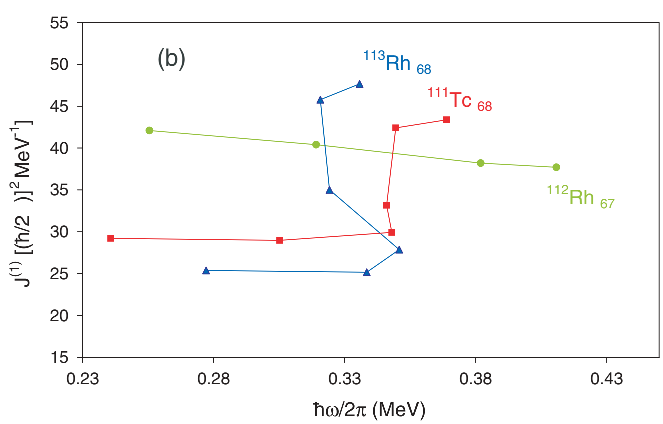

FIG. 6(b). (Color online) Kinematic moment of inertia $J^{(1)}$ of ground bands of the $N = 68$ isotones ^{111}Tc and ^{113}Rh. $J^{(1)}$ of ^{112}Rh is also shown. Almost the same crossing frequency is observed in these isotones. However, no crossing is seen in ^{112}Rh in the frequency region. Data of ^{112,113}Rh are from [7].

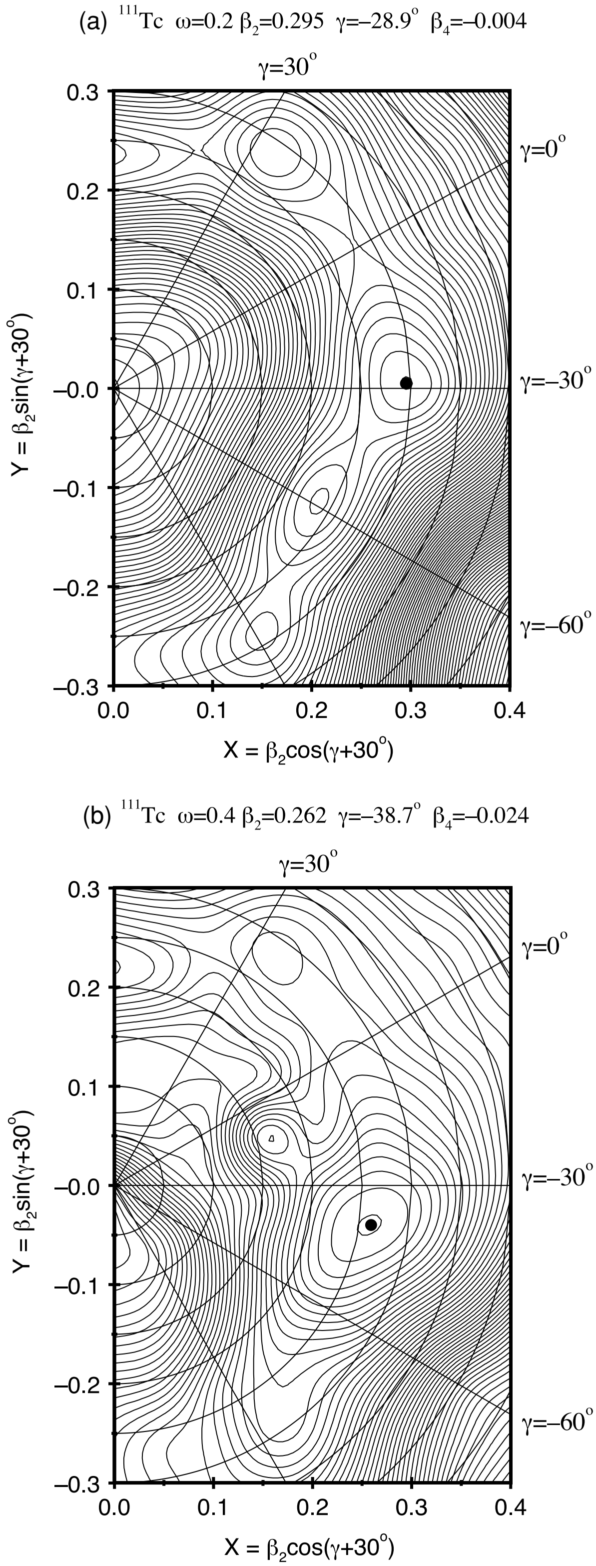

FIG. 7. Polar coordinate plots of total Routhian surface (TRS) calculated at (a) $\hbar\omega = 0.2$ and (b) 0.4 MeV for ^{111}Tc.

be seen in Fig. 7 that a minimum of TRS of ^{111}Tc is observed around deformation parameters $\beta_2 = 0.295$, $\beta_4 = -0.004$, $\gamma = -28.9^\circ$ at $\hbar\omega = 0.2$ MeV and $\beta_2 = 0.262$, $\beta_4 = -0.024$, $\gamma = -38.7^\circ$ at $\hbar\omega = 0.4$ MeV, respectively. Inputting the β_2 and γ parameters obtained in the TRS calculations, the Routhian for ^{111}Tc is calculated by using CSM. An example of the Routhian calculations for ^{111}Tc is presented in Fig. 8 for quasiprotons (a) and quasineutrons (b). One can see that the calculations for ^{111}Tc predict an alignment caused by two $h_{11/2}$ neutrons at a rotational frequency of ~0.36 MeV, which is in good agreement with the observation of the band crossing of ^{111}Tc at ~0.35 MeV, supporting the interpretation of the band crossing as alignment of a pair of $h_{11/2}$ neutrons.

Shown in Fig. 9 are the level systematics of band 6 in ^{105,107,109,111}Tc observed in [8] and in the present work. Those of the Rh isotopes [7] are also given in the figure. A clear tendency is seen in the figure that with increasing neutron number, the excitation energies of the bandhead of band 6 of the Tc isotopes are decreasing, even more rapidly than those in the Rh isotopes. Like the Rh and ^{105,107,109}Tc cases, band 6 of ^{111}Tc, built on the excited $11/2^+$ state, deexcites to the $g_{9/2}$ ground band with predominant feeding to the $9/2^+$ level and very weak decay to the $7/2^+$ level. In view of the low excitation energy of the bandhead and the near vanishing of the $E2$ decay-out transition from the $(11/2^+)$ bandhead to the $7/2^+$ level of the ground band, the γ phonon interpretation for band 6 given in [15] and [22] is unlikely. Instead, as for ^{111,113}Rh [7] and ^{105,107,109}Tc [8], we believe that the level energies and decay pattern of band 6 of ^{111}Tc provide strong evidence of triaxiality. The quenching of the $(11/2^+)_2 \rightarrow 7/2^+_1$transition was explained by examining the wave functions [7]. The main core component in the wave functions of both the initial and final states is the first 2^+ core state; thus the $E2$ transition strength is mainly dictated by the diagonal $E2$ reduced matrix element, which vanishes for $\gamma = -30^\circ$. However, the main core component of the $9/2^+_1$ state is the 0^+ state of the core, resulting in a large $B(E2, 11/2^+_2 \rightarrow 9/2^+_1)$. Band 6 is thus considered to be in the collective family of the ground band, and the term "$K+2$ satellite band" is suggested for it (see discussion in more detail in [8] and in the following paragraphs).

In our previous theoretical calculations dedicated to the investigation of the neutron-rich Y and Nb isotopes [9] and lighter odd-even Tc and Rh isotopes [7,8], we employed the rigid triaxial rotor plus particle (RTRP) model to calculate the energy levels and several $E2$ and $M1$ strengths of the ground bands and some yrare levels. The model described very well the basic properties of these nuclei, such as signature splitting, excitation energies, and branching ratios. In the present work, we describe the level structure of ^{111}Tc in the framework of the same model.

The model was introduced in detail in the paper by Larsson *et al.* [23], and calculations based on this model for several neutron-rich nuclei in the considered mass region can be found in [7–9]. In the RTRP model, the odd particle occupying a deformed single-particle orbital is coupled to a rigid triaxial core. The nuclear field is described by a deformed modified oscillator potential characterized by the deformation parameters ε_2, ε_4, and γ, which are kept constant throughout the calculations (so-called rigid shape). In the present work, a value $\varepsilon_4 = 0$ was assumed. The asymmetry parameter γ was fitted from the splitting of the levels with opposite signature by using the signature-splitting function $S(I)$ suggested by

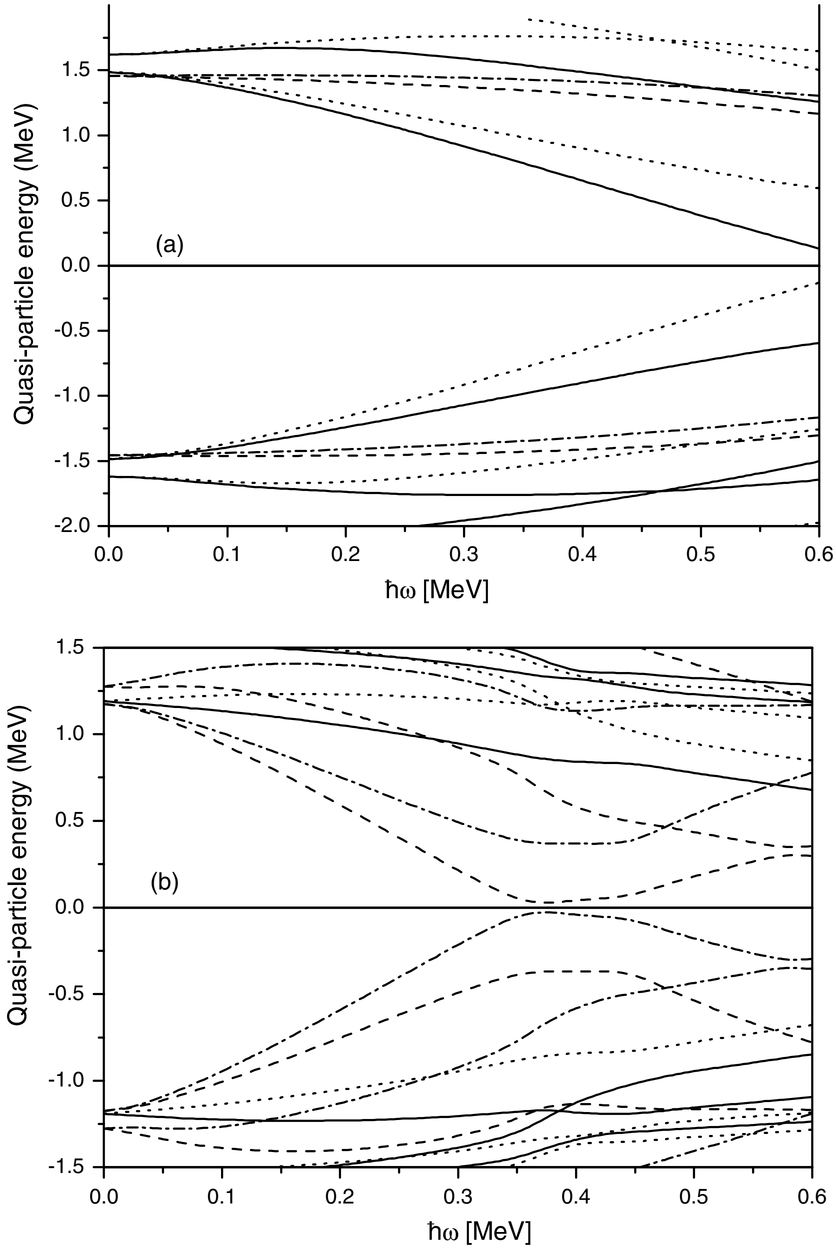

FIG. 8. Calculated Routhian in ^{111}Tc for (a) quasiprotons and (b) quasineutrons plotted vs rotational frequency. The parity and signature (π, α) of the state are solid lines (+,+); dotted lines (+,−); dot-dashed lines (−,+); dashed lines (−,−).

Zamfir *et al.* in Ref. [24], where

$$S(I) = \frac{E(I) - E(I-1)}{E(I) - E(I-2)} \cdot \frac{I(I+1) - (I-2)(I-1)}{I(I+1) - (I-1)I} - 1. \quad (1)$$

We use the Lund convention for γ [25], for which the interval $0 \geqslant \gamma \geqslant -60^\circ$ describes the collective rotation, with $\gamma = 0$ corresponding to a prolate shape and $\gamma = -60^\circ$ corresponding to an oblate shape. The model uses the hydrodynamical irrotational flow formula for the ratios of the moments of inertia along the principal axes, which depend only on the deformation parameter γ. They can be normalized by using the effective value $E(2^+)$ of the core, which represents a scaling factor of the rotational energy. Pairing is included in the model by a standard BCS calculation. It is also possible to reduce the strength of the Coriolis force by an attenuation factor ξ [26]. Because of the triaxiality, the projection K of the total angular momentum I on the intrinsic axis 3 (quantization axis) is no longer equal to the projection Ω of the particle angular momentum J on the same axis. However, in triaxial nuclei, a rotational band can, in principle, be characterized by the K quantum number which has the dominant contribution to the total wave function.

In the case of ^{111}Tc, the fitted parameters are $\varepsilon_2 = 0.32$, $\gamma = -26^\circ$, $E(2^+) = 0.25$ MeV, and $\xi = 0.8$. The RTRP model reproduces very well the large splitting $S(I)$ experimentally found in ^{111}Tc as seen in Fig. 10. In [8], the model parameters found to best fit the shape of ^{107}Tc were $\varepsilon_2 = 0.32$ and $\gamma = -22.5^\circ$. In the present work, RTRP calculations were also performed for ^{109}Tc, and the model parameters found to best fit the shape of ^{109}Tc were $\varepsilon_2 = 0.32$ and $\gamma = -25^\circ$. The RTRP calculations for ^{107,109,111}Tc show that for neutron-rich nuclei with $Z = 43$ in the $A \sim 110$ region,

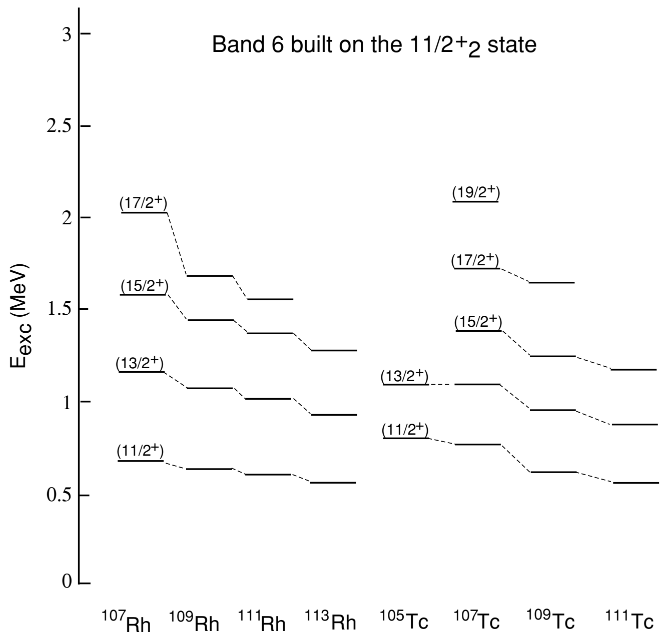

FIG. 9. Level systematics of band 6 of $^{105-111}$Tc and of the Rh isotopes. A rapid lowering of the low-lying bandhead of band 6 with increasing neutron number is observed for both Tc and Rh isotopes. Data are from the present work and [7,8,12,28].

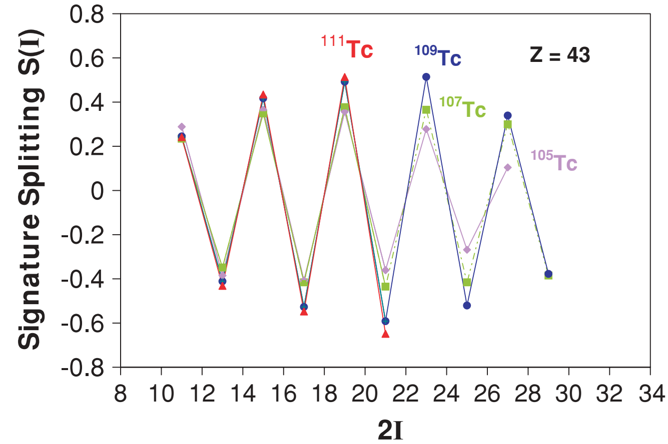

FIG. 11. (Color online) Experimental signature splittings of the ground bands of $^{105-111}$Tc. ◇ ^{105}Tc; □ ^{107}Tc; • ^{109}Tc; ▲^{111}Tc. Signature splitting of ^{111}Tc is the largest among all the Tc isotopes, implying a larger triaxiality. Data are from the present work and [8].

with increasing neutron number, the quadrupole deformation remains practically unchanged while the asymmetry parameter γ becomes larger. The increase in triaxiality with increasing neutron number is in fact suggested by the increase in the signature splitting function when going from ^{105}Tc to ^{111}Tc, as seen in the plot of Fig. 11.

The model also describes quite well the excitation energies of the ground band and yrare band (see Fig. 12). The intrinsic wave functions for the states in both bands were found to be dominated by the $7/2^+[413]$ single-particle orbital. However, as in the case of ^{107}Tc [8], the model does not reproduce the experimental $5/2^+$-$7/2^+$ level ordering, with $5/2^+$ being the ground state. A Harris plot performed for the favored-signature band in ^{107}Tc showed that the $5/2^+$ state clearly deviates from the extrapolated plot, suggesting that the intrinsic structure of this state may be different from that of the rest of the band [8]. In our calculation, the $5/2^+$ level is dominated by a component with $K = 5/2$, while the higher-spin states were found to have a dominant $K = 7/2$ component. In the yrare band, however, the main contribution to the total wave function has $K = 11/2$. The different values of K in bands based on the same Nilsson state are caused by different orientations of the core angular momentum.

The comparison of theoretical and experimental branching ratios $I(I \rightarrow I-1)\,/\,I(I \rightarrow I-2)$ for the transitions within the ground band and the ratio of the decays of the $11/2^+_2$ state $I(11/2^+_2 \rightarrow 9/2^+_1)\,/\,I(11/2^+_2 \rightarrow 7/2^+_1)$ are given in Table III.

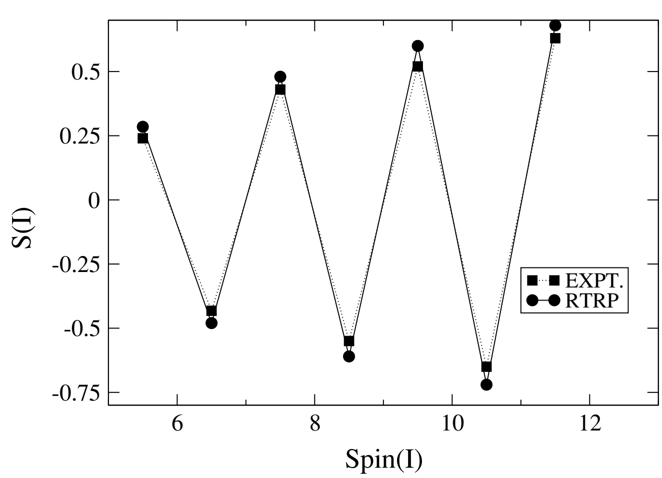

FIG. 10. Comparison of theoretical and experimental signature splitting of the ground band of ^{111}Tc. Calculations were performed using the RTRP model. Good agreement is obtained by using parameters $\varepsilon_2 = 0.32$, $\gamma = -26^\circ$, $E(2^+) = 0.25$ MeV, and $\xi = 0.8$.

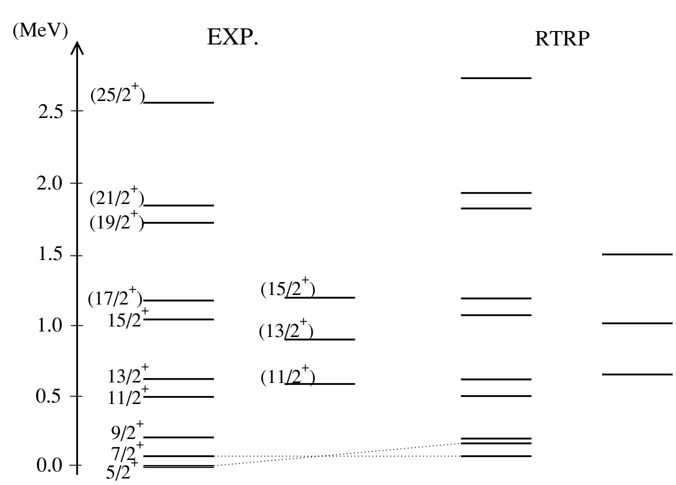

FIG. 12. Comparison of theoretical and experimental excitation energies of the ground band (band 1) and band 6 of ^{111}Tc. Calculations were performed using the RTRP. Good agreement is obtained by using the same parameters as in Fig. 10.

TABLE III. Comparison of theoretical and experimental branching ratios of the ground band and of the decays of band 6 of ^{111}Tc.

Branching ratios	Theory	Expt.
$I(11/2^+ \rightarrow 9/2^+)/I(11/2^+ \rightarrow 7/2^+)$	1.74	2.02
$I(13/2^+ \rightarrow 11/2^+)/I(13/2^+ \rightarrow 9/2^+)$	0.2	0.3
$I(15/2^+ \rightarrow 13/2^+)/I(15/2^+ \rightarrow 11/2^+)$	0.85	1.0
$I(17/2^+ \rightarrow 15/2^+)/I(17/2^+ \rightarrow 13/2^+)$	0.07	0.125
$I(19/2^+ \rightarrow 17/2^+)/I(19/2^+ \rightarrow 15/2^+)$	0.55	1.24
$I(11/2_2^+ \rightarrow 9/2_1^+)/I(11/2_2^+ \rightarrow 7/2_1^+)$	10.8	>13.6

The agreement between experiment and theory is very good. The interesting feature observed in the lighter Tc isotopes, namely, the predominant decay of the $11/2_2^+$ state to the $9/2^+$ state of the ground band, is present also in ^{111}Tc. As a matter of fact, in ^{111}Tc, the $11/2_2^+ \rightarrow 7/2^+$ transition is so weak that its relative intensity could not be extracted in the present experiment. As mentioned above, the preference for the decay of the $11/2_2^+$ to the $9/2_1^+$state was explained by invoking the composition of the core wave functions of the states involved. In ^{111}Tc, for instance, the model predicts that the states $11/2_2^+$, $13/2_2^+$, and $15/2_2^+$ have a dominant$K = 11/2$ component, and the dominant core angular momentum for the $11/2_2^+$ state is $R = 2$. The same core state has the maximum amplitude in the wave function describing the $7/2^+$ state of the ground band, which means that the$E2$ strength of the $11/2_2^+ \rightarrow 7/2^+$ transition is mainly determined by the diagonal matrix element of the quadrupole operator. For nuclei with $\gamma = -30^\circ$, this matrix element vanishes. For the $9/2^+$ state, the calculations reveal that the main contribution to the total wave function is determined by the $R = 0$ core state, resulting in a large matrix element of the quadrupole operator. This property is directly related to the triaxial deformation [27]. If we assume an upper limit of 0.01 relative intensity for the $11/2_2^+ \rightarrow 7/2_1^+$ transition, then the lower limit for the intensity ratio $I(11/2_2^+ \rightarrow 9/2_1^+)$ / $I(11/2+2 \rightarrow 7/2_1^+)$ is 13.6. Theoretically, we obtained 10.8 for the same ratio, which describes rather well the enhancement of the $11/2_2^+ \rightarrow 9/2_1^+$ transition with respect to the $11/2_2^+ \rightarrow 7/2^+$ transition.

Finally, it is necessary to compare the shape parameters used in the CSM and RTRP calculations performed in this work. The CSM calculations reproduced quite well the band crossing of band 1 in ^{111}Tc, and the RTRP calculations gave best fits to the signature splitting, excitations, and branching ratios of the band in the nucleus. Despite the differences in the absolute values of β_2 and γ parameters between CSM and RTRP calculations, the two calculations are in essential agreement, with very large β_2 for the ground band with slowly decreasing deformation with rotational frequency and triaxiality parameter γ that approaches -30° with rotational frequency. We need to keep in mind that the RTRP calculations deal with one-quasiparticle states and are thus only valid within a rotational frequency region below the band crossing. Since in our previous papers, RTRP calculations were performed for the Tc and Rh isotopes [7,8], we prefer to use the shape parameters for ^{111}Tc also obtained via RTRP calculations to study the shape evolutions in the isotopes.

In summary, a high-spin level scheme of ^{110}Tc is established for the first time. Our extension of the level scheme of ^{111}Tc allows the study of band crossing and signature splitting in the more neutron-rich Tc isotopes. The systematics of band-crossing frequencies of the $^{105-111}$Tc isotopes and $N = 68$ Tc/Rh isotones and cranking shell model calculations suggest that the alignment of a pair of $h_{11/2}$ neutrons accounts for the band crossing of the ground band of ^{111}Tc. The very large signature splitting observed in ^{111}Tc (even larger than those observed in $^{105-109}$Tc) is accounted for by large triaxial deformations in the nucleus. A shape of $\varepsilon_2 = 0.32$ and $\gamma = -26^\circ$ is deduced with the best fits to signature splitting, branching ratios, and excitations of the ground band of ^{111}Tc by the RTRP model calculations. This shows an increasing triaxiality with increasing neutron number for Tc isotopes. For ^{110}Tc, a $\Delta I = 1$ band is observed that is similar overall to those in ^{106,108}Tc but shows larger signature splitting and a different sign of signature splitting, with the $I + 4$ level much close to the $I + 5$ level, and similarly for higher spins in ^{110}Tc; while the $I + 4$ level is closer to the $I + 3$ level in ^{106,108}Tc.

The authors are indebted for the use of ^{252}Cf to the office of Basic Energy Sciences, U.S. Department of Energy, through the transplutonium element production facilities at the Oak Ridge National Laboratory. Dr. Augusto Macchiavelli provided valuable help in setting up the Gammasphere electronics for data taking. Dr. Ken Gregorich was instrumental in the design of the source mounting and plastic absorber ball and in mounting the source. The authors also acknowledge the essential help of I. Ahmad, J. Greene, and R. V. F. Janssens in preparing and lending the ^{252}Cf source we used in the year 2000 runs. We greatly appreciate Dr. David Radford's developing and providing the new, less compressed RADWARE cube program.

ACKNOWLEDGMENTS

The work at Vanderbilt University, Lawrence Berkeley National Laboratory, Lawrence Livermore National Laboratory, and Idaho National Laboratory is supported by U.S. Department of Energy under Grant No. DE-FG05-88ER40407 and Contract Nos. W-7405-ENG48, DE-AC03-76SF00098, and DE-AC07-99ID13727. The work at Tsinghua University in Beijing is supported by the Major State Basic Research Development Program under Contract No. G2000077400 and the Chinese National Natural Science Foundation under Grant No. 10375032. The Joint Institute for Heavy Ion Research is supported by its members, U. of Tennessee, Vanderbilt, and the U.S. DOE.

[1] J. Skalski, S. Mizutori, and W. Nazarewicz, Nucl. Phys. **A617**, 282 (1997).
[2] J. H. Hamilton, in *Treatise on Heavy-Ion Science*, edited by D. Allan Bromley (Plenum Press, New York, 1989), Vol. 8, p. 2.
[3] J. H. Hamilton, in *Proceedings of International Symposium on Nuclear Shell Models*, edited by M. Vallieres and B. H.

Wildenthal (World Scientific, Singapore 1985), p. 31; J. H. Hamilton, Prog. Part. Nucl. Phys. **15**, 107 (1985).
[4] K. Becker *et al.*, Z. Phys. A **319**, 193 (1984).
[5] H. Mach *et al.*, Phys. Lett. **B230**, 21 (1989).
[6] M. A. C. Hotchkis *et al.*, Nucl. Phys. **A530**, 111 (1991).
[7] Y. X. Luo *et al.*, Phys. Rev. C **69**, 024315 (2004).
[8] Y. X. Luo *et al.*, Phys. Rev. C **70**, 044310 (2004).
[9] Y. X. Luo *et al.*, J. Phys. G: Nucl. Part. Phys. **31**, 1303 (2005).
[10] M. Bernas *et al.*, Phys. Lett. **B331**, 19 (1994).
[11] J. K. Hwang *et al.*, Phys. Rev. C **57**, 2250 (1998).
[12] A. Bauchet *et al.*, Eur. Phys. J. A **10**, 145 (2001).
[13] K. Li *et al.* (to be submitted for publication).
[14] D. De Frenne and E. Jacobs, Nucl. Data Sheets **89**, 481 (2000).
[15] W. Urban *et al.*, Eur. Phys. J. A **24**, 161 (2005).
[16] S. J. Zhu *et al.* (to be submitted for publication).
[17] J. H. Hamilton *et al.*, Prog. Part. Nucl. Phys. **35**, 635 (1995).
[18] D. C. Radford, Nucl. Instrum. Methods Phys. Res. A **361**, 297 (1995).
[19] R. Bengtsson and S. Frauendorf, Nucl. Phys. **A327**, 139 (1979).
[20] S. Frauendorf, Phys. Lett. **B100**, 219 (1981).
[21] S. Frauendorf and F. R. May, Phys. Lett. **B125**, 245 (1983).
[22] Ts. Venkova *et al.*, Eur. Phys. J. A **15**, 429 (2002).
[23] S. E. Larsson *et al.*, Nucl. Phys. **A307**, 189 (1978).
[24] N. V. Zamfir and R. Casten, Phys. Lett. **B260**, 265 (1991).
[25] S. G. Nilsson and I. Ragnarsson, *Shapes and Shells in Nuclear Structure* (Cambridge University Press, Cambridge, 1995).
[26] P. Ring and P. Schuck, *The Nuclear Many-Body Problem* (Springer-Verlag, 1980).
[27] I. Hamamoto and B. R. Mottelson, Phys. Lett. **B132**, 7 (1983).
[28] Ts. Venkova *et al.*, Eur. Phys. J. A **6**, 405 (1999).